

Shear behavior and analytical model of perfobond connectors

Shuangjie Zheng^{1,2}, Yuqing Liu^{*1}, Teruhiko Yoda² and Weiwei Lin²

¹Department of Bridge Engineering, Tongji University, Shanghai, China

²Department of Civil and Environmental Engineering, Waseda University, Tokyo, Japan

(Received May 28, 2015, Revised July 20, 2015, Accepted July 28, 2015)

Abstract. In steel and concrete composite girders, the load transfer between the steel beam and the concrete slab is commonly ensured by installing shear connectors. In this paper, to investigate the nonlinear behavior of perfobond connectors, a total of 60 push-out specimens were fabricated and tested with the variables for the hole diameter, the concrete strength, the thickness of concrete slab, the diameter, strength and existence of perforating rebar, the thickness, height and distance of perfobond ribs. The failure mode and the load-slip behavior of perfobond connectors were obtained. A theoretical model was put forward to express the load-slip relationship. Analytical formulas of shear capacity and peak slip were also proposed considering the interaction between the concrete dowel and the perforating rebar. The calculation results of the proposals agreed well with the experimental values.

Keywords: composite bridge; perfobond connector; push-out test; load-slip behavior; theoretical model

1. Introduction

Nowadays steel and concrete composite structures have been increasingly used in the construction of both buildings and bridges. The composite action between the steel and concrete components can be ensured by arranging various types of shear connectors, such as headed stud connector (Lin *et al.* 2014), perfobond connector (Cândido-Martins *et al.* 2010), angle connector (Shariati *et al.* 2014) and I-shape connector (Mazoz *et al.* 2013). In practical design, the most extensively used shear connector is the headed stud connector, which resists longitudinal shear and prevents uplift separation between steel and concrete (Oehlers and Coughlan 1986, Johnson 2000, Lee *et al.* 2005, Lin *et al.* 2014). However, the installation of headed stud connectors on site requires specific welding equipment, and the weld may suffer from fatigue problems under cyclic loading (Johnson 2000, Lee *et al.* 2005).

To overcome the drawbacks of the headed stud connector, an alternative connector named perfobond connector was proposed by Leonhardt in the 1980s (Leonhardt *et al.* 1987, Zellner 1987). The perfobond connector consists of a flat steel plate with a number of holes punched through. After concrete casting, dowels formed in the punched holes will resist both the longitudinal shear and the vertical uplift forces. The perfobond connector is easier to install by using continuous fillet welds. Besides, the perfobond connector behaves higher shear stiffness and improved fatigue strength. Therefore, there are increased applications of the perfobond connector in the joints of composite beams (Nakamura *et al.* 2002), composite decks (Kim and Choi 2010), composite

*Corresponding author, Professor, E-mail: yql@tongji.edu.cn

trusses (Liu *et al.* 2013) and hybrid girders (Kim *et al.* 2011).

The bearing mechanism of composite structures is significantly influenced by the connection behavior, which is mostly characterized by the failure mode, shear capacity, slip deformation and load-slip relationship of shear connectors at the steel-concrete interface. Since the earlier research work of Leonhardt *et al.* (1987), Oguejiofor and Hosain (1994), Hosaka *et al.* (2000), Medberry and Shahrooz (2002), Al-Darzi *et al.* (2007), Ahn *et al.* (2010) have investigated the structural behavior of perfobond connectors mainly by push-out tests. It was concluded that the typical failure of perfobond connector was concrete-related. And the shear behavior were significantly influenced by a number of parameters, including the hole diameter, the number of holes, the compressive strength of concrete, the thickness, length and height of the steel plate, the configuration of perforating rebar in the hole and the dimension of concrete slab. Based on the research results, a number of equations were proposed to estimate the shear capacity of perfobond connectors. However, the calculated results of these equations diverge with each other to a great extent, mainly due to the variations in specimen configuration and loading conditions (Hosaka *et al.* 2000, Medberry and Shahrooz 2002, Ahn *et al.* 2010). Besides, other than the suggested equations in *Standard specifications for hybrid structures* (JSCE 2009), few analytical models were reported to calculate the peak slip and to express the load-slip relationship for perfobond connectors.

This paper presents the results of 60 push-out specimens with perfobond connectors. These specimens were designed to investigate the effects of various parameters, including the hole diameter, the concrete strength, the thickness of concrete slab, the diameter, strength and existence of perforating rebar, the thickness, height and distance of perfobond ribs. Based on the experimental results, the failure mode and load-slip behavior of perfobond connectors were obtained. A theoretical model was proposed to express the load-slip relationship. Two calculation methods were put forward to evaluate the shear capacity and the peak slip respectively. Comparisons between the calculation results and the experimental values were performed to verify the proposed equations.

2. Experimental program

2.1 Test specimens

As shown in Table 1, the experimental program consisted of 60 push-out tests divided into 20 groups, each with three identical specimens. The objective was to study the effects of several

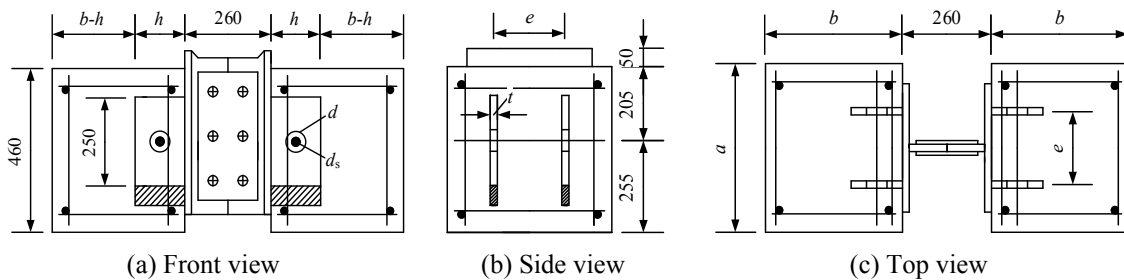


Fig. 1 Details of push-out test specimens (Unit: mm)

parameters, i.e., the hole diameter, the concrete strength, the configuration of perforating rebar, the dimension of perfobond ribs and the geometry of concrete slabs. These specimens were fabricated referencing to the standard push-out test specimen in EN 1994-1-1 (2004). The outlines of the push-out test specimens are illustrated in Fig. 1. As shown in Fig. 1, the specimen of perfobond connector was fabricated in two halves and then connected as a whole by bolts and fish plates before testing. The perforating rebar were all fixed at the center of the hole for each specimen. As listed in Table 1, the geometry parameters were the hole diameter (d), the diameter of perforating rebar (d_s), the thickness (t), height (h) and distance (e) of perfobond ribs, the thickness (b) and width (a) of concrete slabs.

2.2 Material properties

The mechanical properties of concrete and perforating rebar are listed in Table 1. The concrete cube strength (f_{cu}) was obtained from 150-mm concrete cube tests after 28-day air curing period. The uniaxial compressive strength of concrete (f_c) was assumed to be $0.8 f_{cu}$. The secant modulus of concrete was evaluated by using Eq. (1) (FIB 2010).

$$E_c = E_{c0} \alpha_E (f_c/10)^{1/3} \quad (1)$$

Table 1 Push-out test specimens

Group	N_s	d (mm)	d_s (mm)	f_{cu} (MPa)	f_c (MPa)	E_c (GPa)	f_y (MPa)	E_s (GPa)	f_u (MPa)	t (mm)	h (mm)	e (mm)	b (mm)	a (mm)
PS-1	3	50	20	43.3	34.6	32.3	373.6	176.3	577.4	20	150	200	400	460
PS-2	3	60	20	43.3	34.6	32.3	373.6	176.3	577.4	20	150	200	400	460
PS-3	3	75	20	43.3	34.6	32.3	373.6	176.3	577.4	20	150	200	400	460
PS-4	3	50	20	70.3	56.2	38.5	381.7	196.7	546.6	20	150	200	400	460
PS-5	3	60	20	70.3	56.2	38.5	381.7	196.7	546.6	20	150	200	400	460
PS-6	3	75	20	70.3	56.2	38.5	381.7	196.7	546.6	20	150	200	400	460
PS-7	3	60	16	43.3	34.6	32.3	373.6	176.3	577.4	20	150	200	400	460
PS-8	3	60	25	43.3	34.6	32.3	373.6	176.3	577.4	20	150	200	400	460
PS-9	3	60	20	70.3	56.2	38.5	480.0	188.3	623.0	20	150	200	400	460
PS-10	3	60	20	43.3	34.6	32.3	373.6	176.3	577.4	20	100	200	400	460
PS-11	3	60	20	43.3	34.6	32.3	373.6	176.3	577.4	20	150	75	400	460
PS-12	3	60	20	43.3	34.6	32.3	373.6	176.3	577.4	20	150	150	400	460
PS-13	3	65	20	43.3	34.6	32.3	373.6	176.3	577.4	16	210	200	400	460
PS-14	3	65	20	43.3	34.6	32.3	373.6	176.3	577.4	22	210	200	400	460
PS-15	3	60	20	43.3	34.6	32.3	373.6	176.3	577.4	20	150	200	300	460
PS-16	3	75	20	63.4	50.7	36.3	335.0	200.0	455.0	20	150	150	500	400
PS-17	3	50	20	54.6	43.7	35.4	335.0	200.0	455.0	20	100	150	200	400
PS-18	3	50	20	54.6	43.7	35.4	335.0	200.0	455.0	20	100	150	200	400
PS-19	3	50	20	54.6	43.7	35.4	335.0	200.0	455.0	20	100	150	200	400
PS-20	3	50	—	54.6	43.7	35.4	335.0	200.0	455.0	20	100	150	200	400



Fig. 2 Test setup

where E_c is the secant modulus of concrete (GPa); $E_{c0} = 21.5$ GPa; $\alpha_E = 1.0$ for quartzite aggregates.

According to tension tests, the mean yield strength (f_y) and tensile strength (f_u) of perforating rebar were obtained. The yield strength and tensile strength of the steel beam were 410.0 MPa and 545.0 MPa, respectively.

2.3 Test setup

The push-out test setup for the perfbond connector is shown in Fig. 2. The specimens were loaded statically using a hydraulic jack with a 4000 kN capacity. The first two specimens (denoted as PS-n-1 and PS-n-2) in each group were subjected to monotonic loading. The loading rate was controlled such that failure did not occur in less than 15 min. The third one (labeled as PS-n-3) was tested under uniaxial cyclic loading. Totally seven loading cycles were applied. The maximum load in each cycle was evenly increased from 0.1 to 0.7 times of the average ultimate load of the first two specimens. After these loading cycles, monotonic load was subsequently applied until the specimen failure.

2.4 Measurements

Four linear variable differential transformers (LVDTs) were symmetrically mounted at the front and back sides of each specimen. During the test, the applied load and relative slip between steel and concrete were continuously recorded.

3. Test results

3.1 General

Table 2 summarizes the shear capacity of each specimen ($V_{u,i}$), average shear capacity of each group ($V_{u,Avg}$), peak slip corresponding to the shear capacity ($s_{p,i}$), average peak slip of each group ($s_{p,Avg}$), characteristic resistance ($V_{u,k}$), slip capacity ($s_{u,i}$) and characteristic slip capacity ($s_{u,k}$). The

Table 2 Push-out test results

Specimen	$V_{u,i}$ (kN)	$V_{u,Avg}$ (kN)	$s_{p,i}$ (mm)	$s_{p,Avg}$ (mm)	$V_{u,k}$ (kN)	$s_{u,i}$ (mm)	$s_{u,k}$ (mm)	Specimen	$V_{u,i}$ (kN)	$V_{u,Avg}$ (kN)	$s_{p,i}$ (mm)	$s_{p,Avg}$ (mm)	$V_{u,k}$ (kN)	$s_{u,i}$ (mm)	$s_{u,k}$ (mm)
	1 328.0		3.22			8.32		1 335.3		3.61				8.19	
PS-1	2 306.9	316.4	3.28	3.39	276.2	9.74	7.49	PS-11	2 333.8	338.9	3.48	3.71	300.4	8.84	7.37
	3 314.3		3.68			9.84		3 347.5		4.03				9.71	
	1 335.3		3.53			9.85		1 362.7		4.07				9.86	
PS-2	2 329.0	332.1	4.14	3.84	296.1	9.90	8.87	PS-12	2 358.3	346.6	3.50	3.80	286.8	8.82	7.94
	3 332.0		3.85			9.85		3 318.7		3.82				9.18	
	1 386.2		3.86			9.81		1 392.6		4.55				9.44	
PS-3	2 333.8	357.8	4.43	4.49	300.4	9.07	8.83	PS-13	2 394.5	393.7	5.03	5.01	353.3	9.21	8.29
	3 353.4		5.18			9.87		3 394.0		5.45				9.84	
	1 386.9		3.13			9.79		1 374.0		3.27				9.84	
PS-4	2 430.5	394.1	2.95	3.04	328.4	9.84	6.52	PS-14	2 415.6	404.0	3.13	3.16	336.6	8.61	7.75
	3 364.9		3.03			7.25		3 422.4		3.08				9.76	
	1 420.0		3.86			9.87		1 323.6		3.81				9.40	
PS-5	2 438.5	424.0	3.25	3.48	372.2	9.88	8.81	PS-15	2 334.6	326.8	4.22	3.92	289.9	9.94	7.48
	3 413.5		3.33			9.79		3 322.1		3.74				8.31	
	1 523.6		4.17			9.75		1 494.1		2.79				3.05	
PS-6	2 540.1	514.4	4.68	4.42	431.6	9.90	8.78	PS-16	2 474.9	494.7	2.48	2.64	427.4	6.34	2.75
	3 479.5		4.41			9.70		3 515.0		—				—	
	1 284.9		3.37			8.68		1 340.7		2.18				2.21	
PS-7	2 284.4	289.5	3.94	3.53	256.0	8.18	7.36	PS-17	2 320.0	364.9	0.36	1.43	288.0	0.38	0.34
	3 299.1		3.28			9.06		3 434.0		1.74				1.77	
	1 397.0		5.55			9.74		1 362.8		1.62				2.89	
PS-8	2 346.1	372.8	5.18	5.22	311.5	9.61	7.84	PS-18	2 375.9	359.3	1.32	1.50	305.3	1.34	1.21
	3 375.4		4.94			8.71		3 339.2		1.56				1.58	
	1 440.0		3.34			9.88		1 363.0		1.89				1.90	
PS-9	2 466.0	453.3	3.22	3.42	396.0	9.68	8.46	PS-19	2 351.0	358.7	1.91	1.86	315.9	1.93	1.62
	3 454.0		3.70			9.40		3 362.2		1.78				1.80	
	1 350.5		3.75			8.19		1 204.7		0.65				0.67	
PS-10	2 317.1	329.6	3.88	3.93	285.4	4.19	3.77	PS-20	2 167.2	203.1	0.57	0.57	150.5	0.94	0.60
	3 321.1		4.17			9.57		3 237.5		0.48				1.47	

shear capacity (V_u) is defined as the maximum load per hole during the tests. The peak slip (s_p) is the slip corresponding to the shear capacity (V_u). According to EN 1994-1-1 (2004), the characteristic resistance ($V_{u,k}$) is taken as the minimum shear capacity reduced by 10%, the slip capacity ($s_{u,i}$) of each specimen is determined as the maximum slip measured at the characteristic load level, and the characteristic slip capacity ($s_{u,k}$) is taken as the minimum test value of slip capacity reduced by 10%.

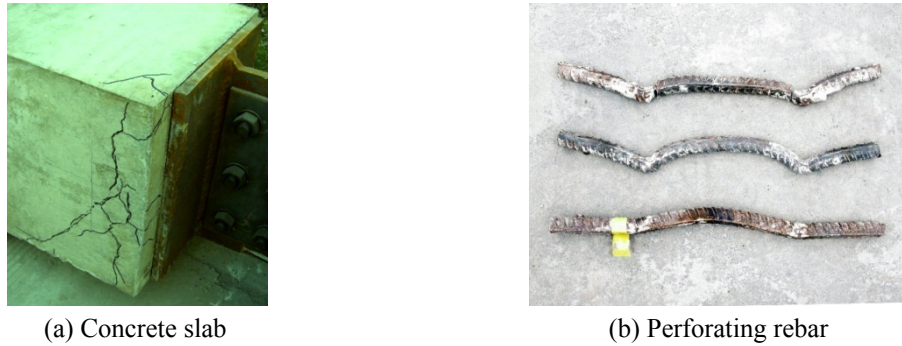


Fig. 3 Failure in the concrete slab and perforating rebar



Fig. 4 Failure in the concrete dowel

3.2 Failure modes

The failure modes of all the specimens were characterized by failure in the concrete. The initial crack in the concrete slab appeared close to the position of perfobond connectors. As presented in Fig. 3, the crack spread out toward the top and bottom of the concrete slab, and the perforating rebar yielded at the locations of perforation after the loading. Fig. 4 shows the failure mode of the concrete dowel in the hole and no obvious deformation was found in the steel beam and perfobond ribs.

3.3 Load-slip behavior

As the applied load increased, the slip between the steel beam and the concrete slab occurred. The measured load-slip curves of perfobond connectors are shown in Fig. 5. The envelope of load-slip curve under uniaxial cyclic loading was close to that under monotonic loading. The shear load (V) was taken as the applied load per hole. The relative slip (s) was obtained by averaging the output of the four LVDTs in each specimen. As shown in Fig. 5, the typical load-slip curves of perfobond connectors consisted of three parts. The initial part of these curves was almost linear with very small slips, which indicated elastic behavior and large shear stiffness. The second part of the load-slip curves was a nonlinear branch. Before the slip increased to the peak slip, the shear load increased slowly and the shear stiffness reduced continuously. At the post-failure stage, the perfobond connector was able to sustain a great amount of residual shear load.

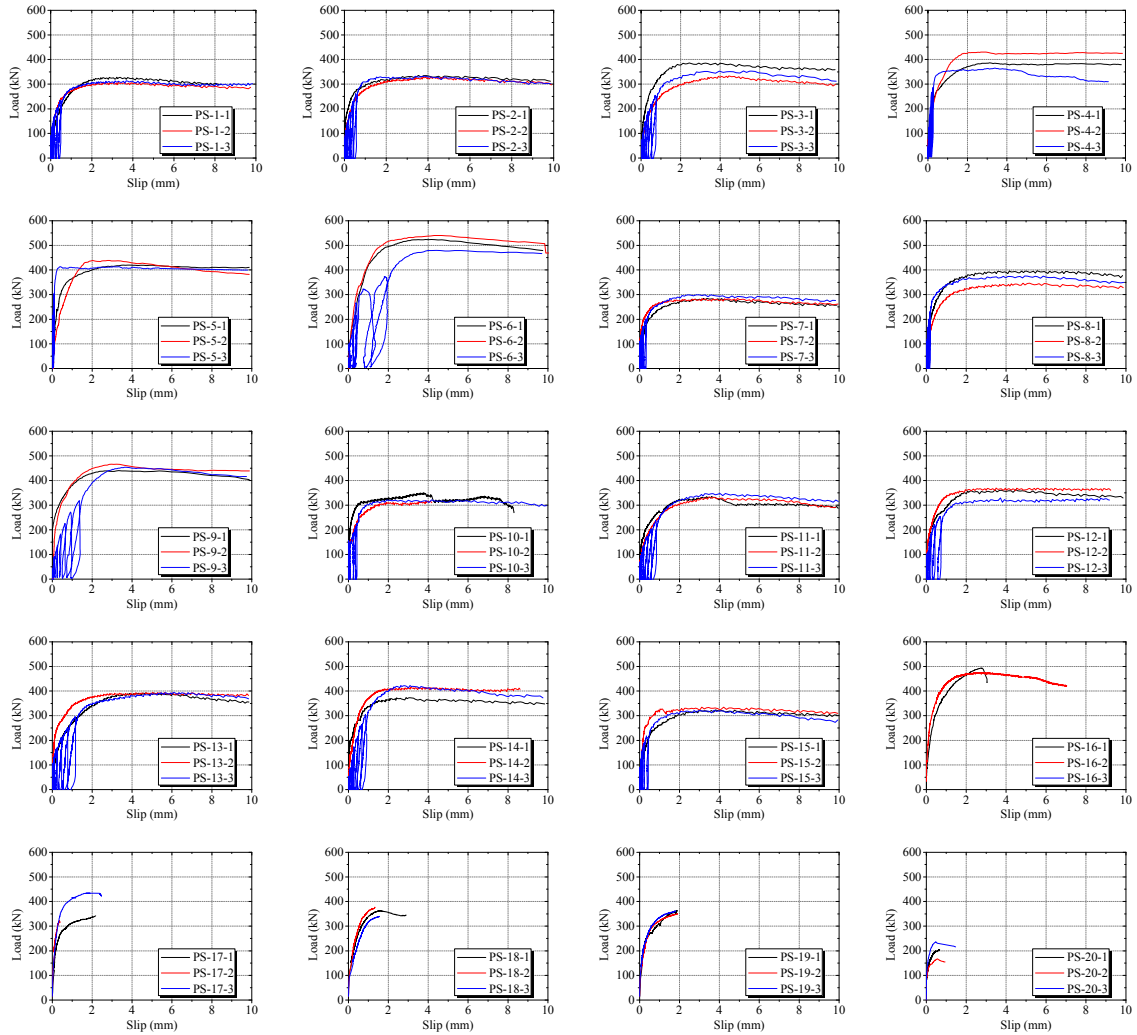


Fig. 5 Load-slip curves

4. Discussion

The connection behavior of composite bridges mainly depends on the load-slip behavior of shear connectors arranged at the steel and concrete interface. This load-slip behavior, usually obtained from push-out tests, depends on the type and dimensions of shear connectors, the configuration of reinforcements and the material properties. A number of parameters that affect the load-slip behavior of perfbond connectors are discussed in the following sections.

4.1 Effect of hole diameter

The hole diameters of perfbond connector in groups PS-1, PS-2 and PS-3 were 50 mm, 60 mm and 75 mm, respectively. As shown in Fig. 6, the hole diameter had obvious influences on both the

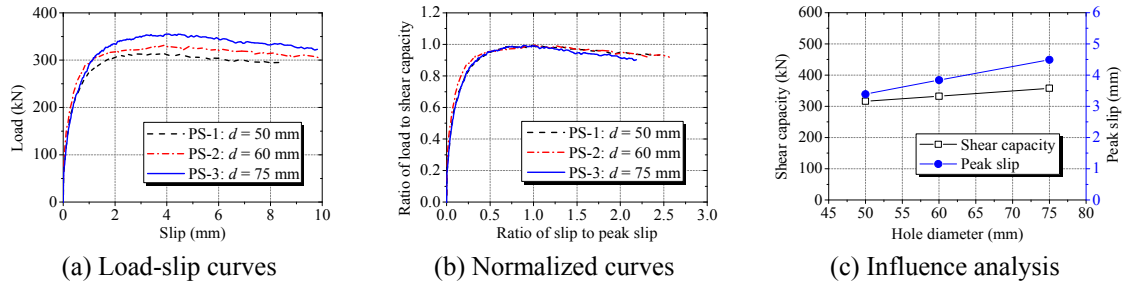


Fig. 6 Effect of hole diameter

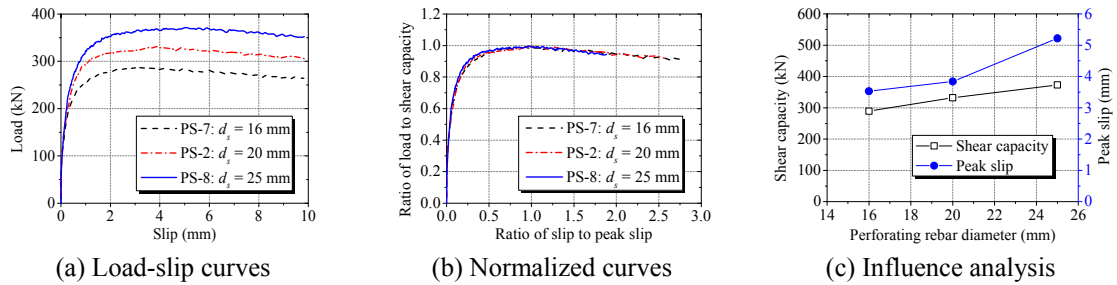


Fig. 7 Effect of perforating rebar diameter

shear capacity and peak slip of perfobond connectors. When the hole diameter increased from 50 mm to 60 mm, the shear capacity and peak slip of perfobond connectors increased by 5% and 13%, respectively. The increase of the hole diameter from 50 mm to 75 mm led to a 13% increase in the shear capacity and a 32% increase in the peak slip of perfobond connector. As illustrated in Fig. 6(b), the hole diameter had negligible effect on the shape of normalized load-slip curves.

4.2 Effect of perforating rebar diameter

The specimens in groups PS-7, PS-2 and PS-8 were identical except that the diameters of the perforating rebar were 16 mm, 20 mm and 25 mm respectively. As presented in Fig. 7, the shear capacity and peak slip were greatly influenced by changing the perforating rebar diameter. Changing the diameters of perforating rebar from 16 mm to 20 mm and from 16 mm to 25 mm, the shear capacities increased by 15% and 29%, and the corresponding slip deformations increased by 9% and 48%, respectively. The results indicated enhancements in the structural behavior of perfobond connectors by increasing diameter of the perforating rebar. Meanwhile, as revealed in Fig. 7(b), the variations in the perforating rebar diameter had little effect on the shape of normalized curves.

4.3 Effect of concrete strength

The specimens in groups PS-1, PS-2 and PS-3 were identical except that the hole diameter changed from 50 mm, 60 mm to 75 mm. Their corresponding specimens in groups PS-4, PS-5 and PS-6 were designed with the same configuration, except that the concrete cube strength increased from 43.3 MPa to 70.3 MPa. Fig. 8 shows three pairs of load-slip curves of perfobond connectors

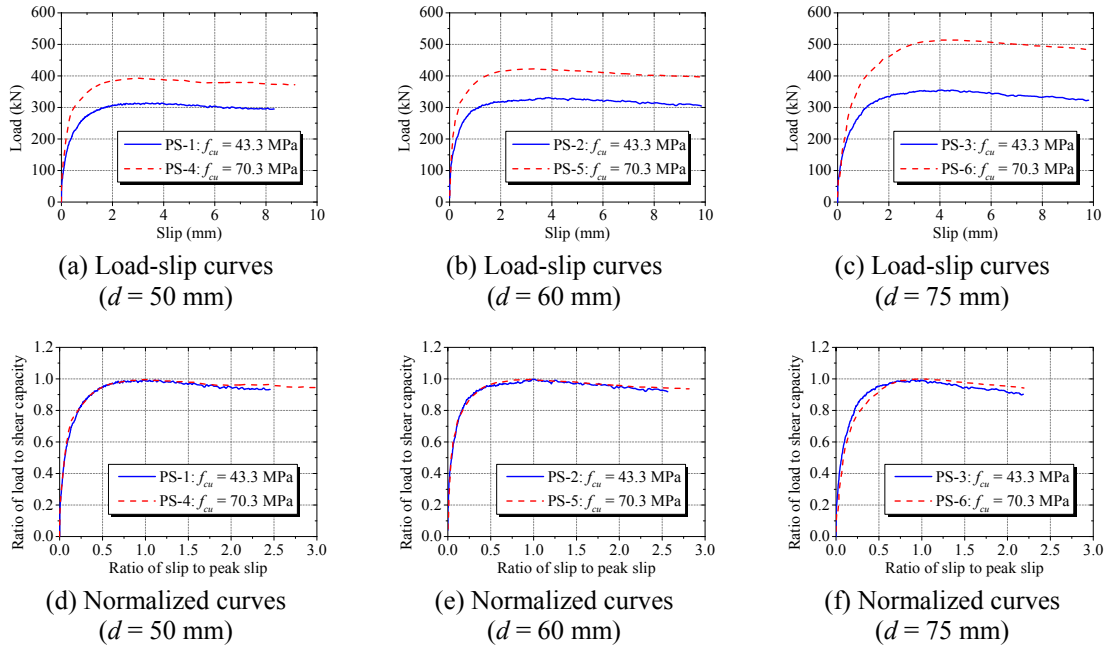


Fig. 8 Effect of concrete strength

with the main variable being the concrete strength and all the other variables being kept constant. The results indicated an increase of the shear capacity and a reduction of the peak slip with increasing the concrete strength. For perfobond connectors with the hole diameter of 50 mm, 60 mm and 75 mm, increasing the concrete strength from 43.3 MPa to 70.3 MPa, the shear capacity increased by 25%, 28% and 44% respectively, while the peak slip reduced by 10%, 9% and 2% respectively. The results revealed that the concrete strength had great effect on the load bearing capacity but slight effect on the normalized curve shape.

4.4 Effect of perforating rebar strength

The specimens in groups PS-5 and PS-9 were identical in configuration except that the yield strengths of the perforating rebar were 381.7 MPa and 480.0 MPa, respectively. As shown in Fig. 9,

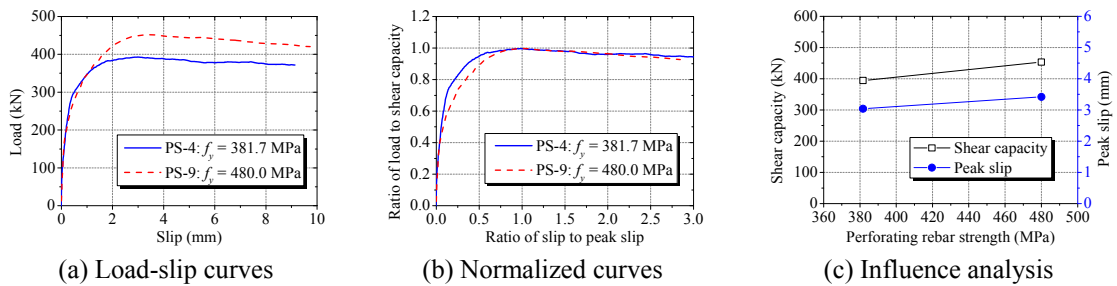


Fig. 9 Effect of perforating rebar strength

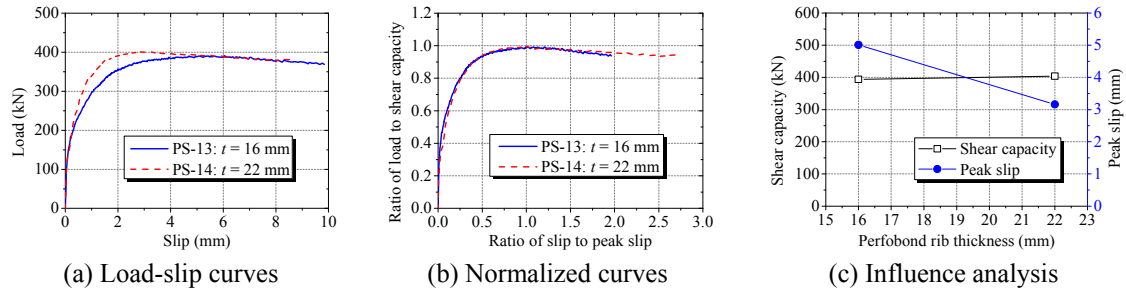


Fig. 10 Effect of perfbond rib thickness

the perforating rebar strength influenced the shear capacity and peak slip of perfbond connectors significantly. Increasing the yield strength of perforating rebar from 381.7 MPa to 480.0 MPa, the shear capacity and peak slip increased by 15% and 13%, respectively. The results revealed that the shear bearing capacity and slip ductility of perfbond connectors were both enhanced by using high-strength rebar in the hole. As illustrated in Fig. 9(b), increasing the perforating rebar strength led to little variations in the shape of normalized load-slip curves.

4.5 Effect of perfbond rib thickness

Fig. 10 presents the load-slip curves and normalized curves of the perfbond connectors with the main variable being the perfbond rib thickness and all the other variables being kept constant. The specimens in groups PS-13 and PS-14 were similar to each other except that the thickness of the perfbond rib were 16 mm and 22 mm, respectively. Increasing the thickness of perfbond rib from 16 mm to 22 mm, the shear capacity increased by 3%, while the peak slip reduced by 37%. The results showed negligible effect on the shear capacity and a reduction of the peak slip with the variation of perfbond rib thickness. As shown in Fig. 10(b), little changes were found in the shape of normalized load-slip curves while changing the thickness of perfbond ribs.

4.6 Effect of perfbond rib height

The load-slip curves and normalized curves of the specimens in groups PS-10 and PS-2 are shown in Fig. 11. These specimens were similar in every respect except that the perfbond rib height varied between 100 mm and 150 mm. The results indicated that the perfbond rib height had

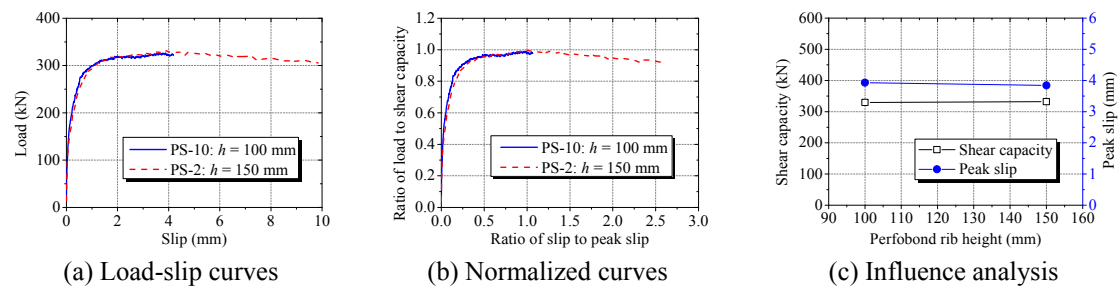


Fig. 11 Effect of perfbond rib height

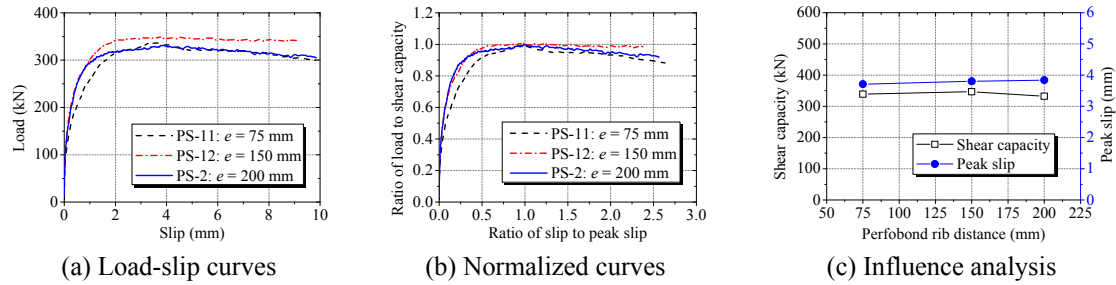


Fig. 12 Effect of perfobond rib distance

little influence on the shear capacity and peak slip of perfobond connectors. With the variation of perfobond rib height from 100 mm to 150 mm, the shear capacity increased by 1% and the peak slip decreased by 2%. As shown in Fig. 11(b), the perfobond rib height had negligible effect on the shape of normalized load-slip curves. The reason might be that the end-bearing effect of the perfobond ribs was removed, and the specimen failure was characterized by the shear of concrete dowel within the punched holes.

4.7 Effect of perfobond rib distance

The specimens in groups PS-11, PS-12 and PS-2 were identical except that the distances of the perfobond ribs were 75 mm, 150 mm and 200 mm respectively. As shown in Fig. 12, the shear capacity and peak slip were slightly affected by the perfobond rib distance. Changing the distances of perfobond ribs among 75 mm, 150 mm and 200 mm, the variations of the shear capacity and the peak slip were less than 2% and 4%, respectively. The results indicated little effect on the structural behavior of perfobond connectors when the perfobond rib distances ranged from 75 mm to 200 mm. The variation of the perfobond rib distance, as presented in Fig. 12(b), had slight influence on the shapes of the normalized load-slip curves.

4.8 Effect of concrete slab thickness

Fig. 13 presents the load-slip curves and normalized curves of the specimens with the main variable being the concrete slab thickness and all the other variables being kept constant. The specimens in groups PS-15 and PS-2 were similar to each other except that the thicknesses of the

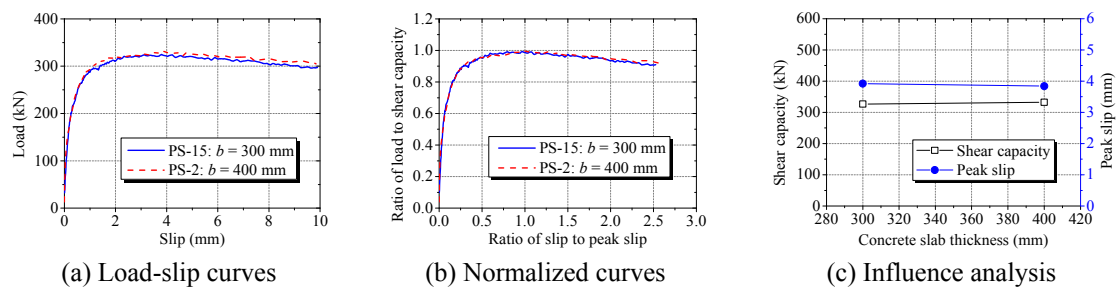


Fig. 13 Effect of concrete slab thickness

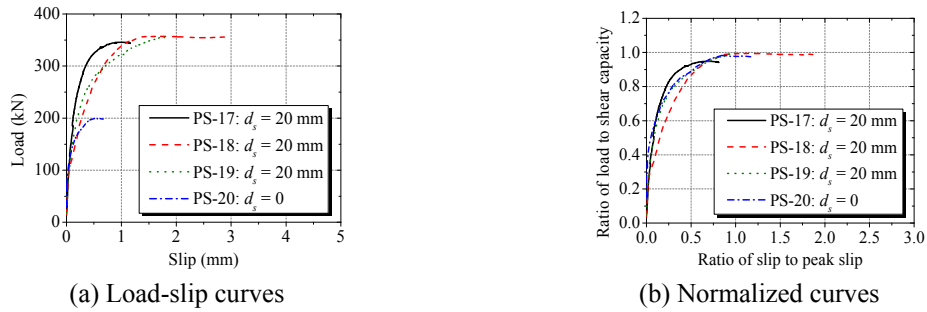


Fig. 14 Effect of perforating rebar existence

concrete slab were 300 mm and 400 mm, respectively. The results revealed that the concrete slab thickness had little effect on the load bearing capacity and slip deformation of perfobond connectors. With the variation of concrete slab thickness from 300 mm to 400 mm, the changes in the shear capacity and the peak slip were both less than 2%. The variation of the concrete slab thickness had negligible effect on the shapes of the normalized load-slip curves, as shown in Fig. 13(b).

4.9 Effect of perforating rebar existence

The load-slip curves and normalized curves of the perfobond connector with and without perforating rebar are shown in Fig. 14. The perfobond ribs of specimens in groups PS-17, PS-18 and PS-19 were perforated with rebar of 20 mm in diameter. On the contrary, no perforating rebar was provided for the specimens in group PS-20. Other than the existence of the perforating rebar, these specimens were similar in the dimensions and materials. As shown in Fig. 14(a), the provision of perforating rebar had great effect on the structural behavior of perfobond connectors. Compared to the specimens without perforating rebar, the shear capacity and the peak slip of specimens with perforating rebar increased by approximately 80% and 180%, respectively. The results indicated that the perforating rebar could significantly enhance the shear bearing capacity and ductility of perfobond connectors. Fig. 14(b) revealed similar patterns of the normalized load-slip curves for perfobond connector with and without perforating rebar.

5. Expression of load-slip relationship

5.1 Existing expression

The shear behavior of perfobond connector has significant influence on the structural response of steel and concrete composite bridges. Under the service loading, typical steel and concrete composite bridges show elastic behavior. The interaction between steel and concrete can be effectively analyzed by using the initial shear stiffness of shear connectors. In the ultimate limit state, the load redistribution occurs among the steel beam, concrete slab and shear connectors in composite bridges. The nonlinear interaction at the steel-concrete interface is greatly affected by the plastic behavior of shear connectors. Therefore, it is important to derive the theoretical load-slip relationship of perfobond connectors.

According to *Standard specifications for hybrid structures* (JSCE 2009), the load-slip curves of perfobond connectors can be expressed in two different conditions. For perfobond connectors with perforating rebar, Eq. (2) was suggested to derive the load-slip relationship. While no perforating rebar was provided in the hole, the empirical load-slip curves can be obtained by using Eq. (3).

$$V/V_u = \begin{cases} \left(1 - e^{-\alpha \cdot s/d_s}\right)^\beta & (0 \leq s \leq s_p) \\ \left(1 - e^{-\alpha \cdot s_p/d_s}\right)^\beta + (2/15)(1 - s/s_p) & (s_p < s \leq 2.5s_p) \end{cases} \quad (2)$$

with $\alpha = 50(t/d)$; $\beta = 1/3$

$$V/V_u = \left(1 - e^{-\alpha_0 \cdot s/d}\right)^\beta \quad (0 \leq s \leq s_p) \quad (3)$$

with $\alpha_0 = 500(t/d)$; $\beta = 1/3$

where V is the shear force carried by one hole of perfobond connector (N); V_u is the shear capacity per hole (N); s is the relative slip between steel and concrete (mm); s_p is the peak slip corresponding to the shear capacity (mm); d is the hole diameter (mm); d_s is the perforating rebar diameter (mm); t is the perfobond rib thickness (mm); α , α_0 and β are fitting coefficients that affect the shape of load-slip curves.

FIB (2010) recommended a dimensionless type of expression, Eq. (4), to fit the experimental load-slip relationships of shear connectors used in steel and concrete composite bridges

$$V/V_u = \left(s/s_p\right)^\gamma \quad (4)$$

where γ is the fitting coefficient that could be obtained from regression analysis of experimental results.

5.2 Proposal

On the basis of 60 push-out test results presented in this study, the load-slip relationships of perfobond connector were mostly influenced by the hole diameter, perforating rebar diameter, concrete strength, perfobond rib thickness and yield strength of perforating rebar. Regardless of the changes in parameters, the shapes of the normalized load-slip curves were similar with each other. Therefore, based on Eq. (4), a modified theoretical model, Eq. (5), was derived to express the load-slip curves of perfobond connectors.

$$V/V_u = (1/15) \left[\left(s/s_p\right)^2 - 10\left(s/s_p\right) + 24\left(s/s_p\right)^{1/3} \right] \quad (5)$$

with $0 \leq s \leq 2.5s_p$ for perfobond connector with perforating rebar
 $0 \leq s \leq s_p$ for perfobond connector without perforating rebar

5.3 Comparison

As shown in Fig. 15, the expressions suggested by JSCE and the proposal in this study were

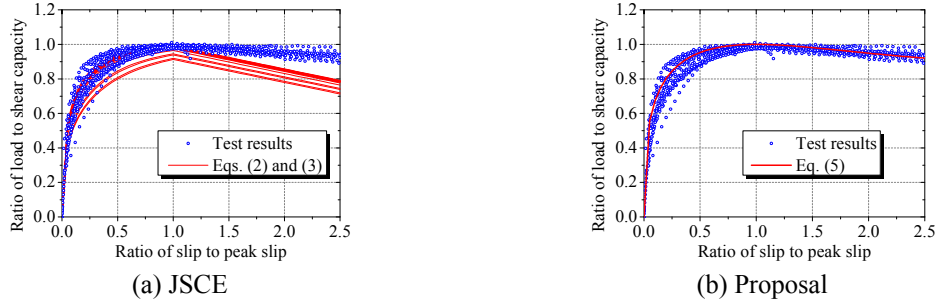


Fig. 15 Experimental results and regression curves

compared with the tested load-slip curves. The comparison in Fig. 15(a) indicated that the expression of Eqs. (2) and (3) agreed reasonably well with the tested curves in the elastic part. However, the shear load was underestimated in the plastic region. The actual shear capacity was unable to be reached by using these exponential functions unless the slip increased to infinitely great. The predicted curves also reduced sharper than the tested results in the descending branch. As shown in Fig. 15(b), the proposed expression, Eq. (5), provided a better prediction of load-slip relationships with the tested curves in different loading stages, including the elastic part, the plastic region and the descending branch as well.

6. Prediction of shear capacity and peak slip

6.1 Shear capacity

In typical load-slip curves, the shear capacity refers to the peak value of shear load, which is a critical parameter that represents the bearing behavior of shear connectors.

On the basis of the earlier experimental work of Leonhardt *et al.* (1987), a calculation method, Eq. (6), was proposed for estimating the shear capacity of perfobond connectors with concrete failure.

$$V_u = 1.4d^2 f_{cu} \quad (6)$$

where V_u is the shear capacity per hole (N); d is the hole diameter (mm); f_{cu} is the concrete cube strength (MPa).

Hosaka *et al.* (2000) carried out push-out tests and developed two shear capacity equations, Eqs. (7) and (8), for perfobond connectors without and with a transverse rebar in the hole, respectively.

$$V_u = 3.38d^2 f_c (t/d)^{1/2} - 39.0 \times 10^3 \quad (7)$$

with $22.0 \times 10^3 < d^2 f_c (t/d)^{1/2} < 194.0 \times 10^3$

$$V_u = 1.45 \left[(d^2 - d_s^2) f_c + d_s^2 f_u \right] - 26.1 \times 10^3 \quad (8)$$

with $51.0 \times 10^3 < (d^2 - d_s^2) f_c + d_s^2 f_u < 488.0 \times 10^3$

where t is the perfobond rib thickness (mm); d_s is the diameter of the perforating rebar (mm); f_c is

the concrete cylinder strength (MPa); f_u is the tensile strength of the perforating rebar (MPa).

The interaction between the concrete dowel and the perforating rebar had great effects on the shear capacity of perfobond connector, as revealed in the experimental results. The effect of the concrete dowel was considered in Eq. (6). The contributions of the concrete dowel and the perforating rebar were taken into account separately in Eqs. (7) and (8).

Based on the push-test results and previous proposals as Eqs. (6)-(8), the concrete dowel force of perfobond connectors is related to $d^2 f_c$. The interaction between the concrete dowel and the perforating rebar depends on the connector size and material properties, which can be effectively considered by multiplying an interaction factor. Therefore, the equation for predicting the shear capacity of perfobond connector can be expressed in the following form

$$V_u = C_1 d^2 f_c \left[1 + C_2 (d_s/d)^{\alpha_1} (f_y/f_c)^{\alpha_2} \right] \quad (9)$$

where f_c is the concrete cylinder strength (MPa); f_y is the yield strength of the perforating rebar (MPa); C_1 , C_2 , α_1 and α_2 are fitting coefficients.

By using nonlinear least square curve fitting methods, the coefficients in Eq. (9) were obtained from the test results as follows: $C_1 = 1.35$, $C_2 = 7.06$, $\alpha_1 = 3$ and $\alpha_2 = 1/2$. Therefore, the shear capacity of perfobond connector can be obtained by Eq. (10).

$$V_u = 1.35 d^2 f_c \left[1 + 7.06 (d_s/d)^3 (f_y/f_c)^{1/2} \right] \quad (10)$$

6.2 Peak slip

The peak slip is an important parameter that reflects the ductility of shear connector in steel and concrete composite bridges. However, little research has been found to provide calculation methods for predicting the peak slip of perfobond connector.

JSCE (2009) recommended two equations, Eqs. (11) and (12), to estimate the peak slip of perfobond connector. The first equation, Eq. (11), was suggested to calculate the peak slip of perfobond connector without perforating rebar. When rebar was provided in the punched hole, Eq. (12) could be used to calculate the peak slip.

$$s_p = 0.006d(d/t) \quad (11)$$

$$s_p = 0.067d_s(d/t) \quad (12)$$

where s_p is the peak slip corresponding to the shear capacity (mm); d is the hole diameter (mm); d_s is the perforating rebar diameter (mm); t is the perfobond rib thickness (mm).

The results indicated that the peak slip of perfobond connector was significantly influenced by the hole diameter, the perforating rebar diameter, the concrete strength, the yield strength of perforating rebar and the perfobond rib thickness. Eqs. (11) and (12) considered the effects of the hole diameter, the perforating rebar diameter and the perfobond rib thickness, but neglected the influence of the material properties.

On the basis of the test results, the peak slip of perfobond connector included the contributions of the concrete dowel and the perforating rebar. The expression for calculating the peak slip of perfobond connector can be assumed as below

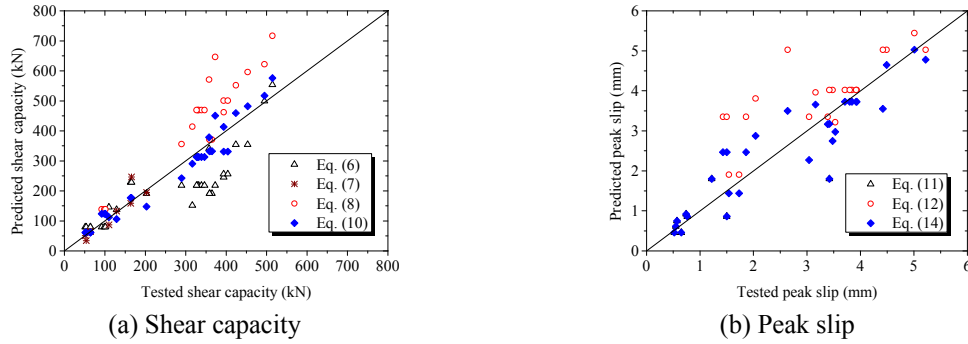


Fig. 16 Comparison of shear capacity and peak slip equations

$$s_p = D_1 d (d/t) \left[1 + D_2 (d_s/d)^{\beta_1} (f_y/f_c)^{\beta_2} \right] \quad (13)$$

where f_c is the concrete cylinder strength (MPa); f_y is the yield strength of the perforating rebar (MPa); D_1 , D_2 , β_1 , and β_2 are fitting coefficients.

Nonlinear regression analysis on the test results was carried out and the coefficients in Eq. (13) were determined as follows: $D_1 = 0.006$, $D_2 = 1.18$, $\beta_1 = 3/2$, and $\beta_2 = 1$. Therefore, the peak slip of perfobond connector can be provided by Eq. (14).

$$s_p = 0.006d(d/t) \left[1 + 1.18(d_s/d)^{3/2} (f_y/f_c) \right] \quad (14)$$

6.3 Verification

The proposed equations, Eqs. (10) and (14), were validated by comparing the above equations with the tested shear capacity and peak slip. Table 3 summarizes the general data of the push-out

Table 3 Push-out test data

Group	N_s	d (mm)	t (mm)	f_c (MPa)	d_s (mm)	f_y (MPa)	f_u (MPa)	$V_{u,test}$ (kN)	$S_{p,test}$ (mm)	References
C-12-140-L	1	60	12	23.1	—	—	—	110.0	3.42	Furuichi <i>et al.</i> (1998)
C-12-140-H	1	60	12	36.3	—	—	—	164.0	1.22	
C-25-140-L	1	60	25	21.8	—	—	—	129.0	1.50	
C-25-140-H	1	60	25	36.3	—	—	—	166.0	0.76	
Type 1	3	35	16	37.0	—	—	—	63.9	0.52	Hosaka <i>et al.</i> (2000)
Type 2	3	35	16	37.0	13	295.0	440.0	92.1	1.73	
Type 3	3	35	12	37.0	—	—	—	51.4	0.55	
Type 4	3	35	8	37.0	—	—	—	53.8	0.74	
Type 5	3	35	8	37.0	13	295.0	440.0	98.7	2.04	
Type 6	3	35	16	37.0	—	—	—	64.1	0.65	
Type 7	3	35	16	37.0	13	295.0	440.0	101.2	1.54	

Table 4 Calculated results

Group	Shear capacity (kN)					Peak slip (mm)				References
	Test	Eq. (6)	Eq. (7)	Eq. (8)	Eq. (10)	Test	Eq. (11)	Eq. (12)	Eq. (14)	
C-12-140-L	110.0	151.6	86.7	—	112.3	3.42	1.80	—	1.80	Furuichi <i>et al.</i> (1998)
C-12-140-H	164.0	218.2	158.5	—	176.4	1.22	1.80	—	1.80	
C-25-140-L	129.0	341.0	132.2	—	105.9	1.50	0.86	—	0.86	
C-25-140-H	166.0	246.1	246.1	—	176.4	0.76	0.86	—	0.86	
Type 1	63.9	354.3	64.6	—	61.2	0.52	0.46	—	0.46	Hosaka <i>et al.</i> (2000)
Type 2	92.1	553.6	—	138.4	123.7	1.73	—	1.91	1.44	
Type 3	51.4	218.2	50.7	—	61.2	0.55	0.61	—	0.61	
Type 4	53.8	218.2	34.2	—	61.2	0.74	0.92	—	0.92	
Type 5	98.7	354.3	—	138.4	123.7	2.04	—	3.81	2.88	
Type 6	64.1	218.2	64.6	—	61.2	0.65	0.46	—	0.46	
Type 7	101.2	218.2	—	138.4	123.7	1.54	—	1.91	1.44	
PS-1	316.4	218.2	—	414.1	290.2	3.39	—	3.35	3.17	This study
PS-2	332.1	256.1	—	469.3	312.6	3.84	—	4.02	3.73	
PS-3	357.8	256.1	—	570.9	378.3	4.49	—	5.03	4.65	
PS-4	394.1	218.2	—	462.1	413.0	3.04	—	3.35	2.27	
PS-5	424.0	499.3	—	551.7	459.3	3.48	—	4.02	2.75	
PS-6	514.4	191.1	—	716.7	575.7	4.42	—	5.03	3.55	
PS-7	289.5	191.1	—	356.0	242.1	3.53	—	3.22	2.97	
PS-8	372.8	191.1	—	646.4	450.4	5.22	—	5.03	4.78	
PS-9	453.3	79.4	—	596.0	481.9	3.42	—	4.02	3.17	
PS-10	329.6	79.4	—	469.3	312.6	3.93	—	4.02	3.73	
PS-11	338.9	79.4	—	469.3	312.6	3.71	—	4.02	3.73	
PS-12	346.6	191.1	—	469.3	312.6	3.80	—	4.02	3.73	
PS-13	393.7	145.7	—	500.7	330.7	5.01	—	5.44	5.03	
PS-14	404.0	228.8	—	500.7	330.7	3.16	—	3.96	3.66	
PS-15	326.8	137.6	—	469.3	312.6	3.92	—	4.02	3.73	
PS-16	494.7	228.8	—	621.9	517.5	2.64	—	5.03	3.50	
PS-17	364.9	79.4	—	370.9	332.0	1.43	—	3.35	2.47	
PS-18	359.3	79.4	—	370.9	332.0	1.50	—	3.35	2.47	
PS-19	358.7	79.4	—	370.9	332.0	1.86	—	3.35	2.47	
PS-20	203.1	79.4	194.5	—	147.5	0.57	0.75	—	0.75	

tests in references which adopt similar specimen configuration. Table 4 presents the calculated results according to the existing equations and the proposal in this study.

Fig. 16 presents the comparison of different equations for predicting the shear capacity and peak slip of perfobond connectors. As shown in Fig. 16(a), with the increase of the shear capacity, Eq. (6) tended to be on the conservative side, while Eq. (8) might overestimate the experimental

results. The reason may be that the effect of the perforating rebar was not included in Eq. (6). And the contribution of perforating rebar was overestimated in Eq. (8) by using the tensile strength of rebar. A better prediction of the shear capacity could be obtained by Eq. (10) proposed in this study. Compared to existing formulas, the proposed Eq. (14) also presented less scattering results for calculating the peak slip of perfobond connector, as revealed in Fig. 16(b).

7. Conclusions

Based on 60 push-out tests of perfobond connectors, the following conclusions can be drawn:

- The typical load-slip curves of perfobond connectors consisted of elastic, plastic and descending parts. For perfobond connectors with perforating rebar in the holes, a great amount of shear load was sustained at post-failure stage. When no rebar was provided in the holes, the descending branch of load-slip curves was not evident.
- The effects of a number of parameters on the structural behavior of perfobond connectors were investigated. The results indicated that the shear capacity and slip ductility were significantly influenced by the hole diameter, perforating rebar diameter, concrete strength, perforating rebar strength and the perfobond rib thickness.
- A theoretical load-slip relationship was developed for perfobond connectors with and without perforating rebar in the holes. When rebar was provided in the hole, the ultimate slip was taken as 2.5 times of the peak slip. For perfobond connectors without perforating rebar, the slip deformation was assumed to be no greater than the peak slip.
- Two analytical models were proposed to predict the shear capacity and the peak slip of perfobond connectors respectively. The effect of material properties and the interaction between the concrete dowel and the perforating rebar were considered. The calculation results agreed reasonably well with the experimental values.

All the findings in this study may provide references for the application of perfobond connectors in steel and concrete composite structures.

References

- Ahn, J.H., Lee, C.G., Won, J.H. and Kim, S.H. (2010), "Shear resistance of the perfobond-rib shear connector depending on concrete strength and rib arrangement", *J. Constr. Steel Res.*, **66**(10), 1295-1307.
- Al-Darzi, S.Y.K., Chen, A.R. and Liu, Y.Q. (2007), "Finite element simulation and parametric studies of perfobond rib connector", *Am. J. Appl. Sci.*, **4**(3), 122-127.
- Cândido-Martins, J.P.S., Costa-Neves, L.F. and Vellasco, P.C.G.S. (2010), "Experimental evaluation of the structural response of Perfobond shear connectors", *Eng. Struct.*, **32**(8), 1976-1985.
- EN 1994-1-1 (2004), Eurocode 4: Design of composite steel and concrete structures, Part 1-1: General rules and rules for buildings, European Committee for Standardisation (CEN), Brussels, Belgium.
- FIB (2010), FIB bulletin 65: Model code 2010 – Final draft, (Volume 1), International Federation for Structural Concrete, Lausanne, Switzerland.
- Furuichi, K., Taira, Y. and Yamamura, M. (1998), "Experimental study on shear strength of shear connectors using perforated plate", Annual Report; Kajima Technical Research Institute No. 46, Tokyo, Japan.
- Hosaka, T., Mitsuki, K., Hiragi, H., Ushijima, Y., Tachibana, Y. and Watanabe, H. (2000), "An experimental study on shear characteristics of perfobond strip and its rational strength equations", *J.*

- Struct. Eng., JSCE*, **46A**, 1593-1604.
- Johnson, R.P. (2000), "Resistance of stud shear connectors to fatigue", *J. Constr. Steel Res.*, **56**(2), 101-116.
- JSCE (2009), Standard specifications for hybrid structures, Japan Society of Civil Engineers, Tokyo, Japan.
- Kim, S.H. and Choi, J.H. (2010), "Experimental study on shear connection in unfilled composite steel grid bridge deck", *J. Constr. Steel Res.*, **66**(11), 1339-1344.
- Kim, S.H., Lee, C.G., Ahn, J.H. and Won, J.H. (2011), "Experimental study on joint of spliced steel-PSC hybrid girder, part I: proposed parallel-perfobond-rib-type joint", *Eng. Struct.*, **33**(8), 2382-2397.
- Lee, P.G., Shim, C.S. and Chang, S.P. (2005), "Static and fatigue behavior of large stud shear connectors for steel-concrete composite bridges", *J. Constr. Steel Res.*, **61**(9), 1270-1285.
- Leonhardt, F., Andrä, W., Andrä, H.P. and Harre, W. (1987), "Neues, vorteilhaftes Verbundmittel für Stahlverbund-Tragwerke mit hoher Dauerfestigkeit", *Beton-und Stahlbetonbau*, **82**(12), 325-331.
- Lin, Z., Liu, Y. and He, J. (2014), "Behavior of stud connectors under combined shear and tension loads", *Eng. Struct.*, **81**, 362-376.
- Liu, Y., Xin, H., He, J., Xue, D. and Ma, B. (2013), "Experimental and analytical study on fatigue behavior of composite truss joints", *J. Constr. Steel Res.*, **83**, 21-36.
- Mazoz, A., Benanane, A. and Titoum, M. (2013), "Push-out tests on a new shear connector of I-shape", *Int. J. Steel Struct.*, **13**(3), 519-528.
- Medberry, S.B. and Shahrooz, B.M. (2002), "Perfobond shear connector for composite construction", *Eng. J. AISC*, **39**(1), 2-12.
- Nakamura, S., Momiyama, Y., Hosaka, T. and Homma, K. (2002), "New technologies of steel/concrete composite bridges", *J. Constr. Steel Res.*, **58**(1), 99-130.
- Oehlers, D.J. and Coughlan, C.G. (1986), "The shear stiffness of stud shear connections in composite beams", *J. Constr. Steel Res.*, **6**(4), 273-284.
- Oguejiofor, E.C. and Hosain, M.U. (1994), "A parametric study of perfobond rib shear connectors", *Can. J. Civil Eng.*, **21**(4), 614-625.
- Shariati, A., Shariati, M., Ramli Sulong, N.H., Suhatri, M., Arabnejad Khanouki, M.M. and Mahoutian, M. (2014), "Experimental assessment of angle shear connectors under monotonic and fully reversed cyclic loading in high strength concrete", *Con. Build. Mater.*, **52**, 276-283.
- Zellner, W. (1987), "Recent designs of composite bridges and a new type of shear connectors", *Proceedings of the ASCE Engineering Foundation Conference on Composite Construction*, Henniker, NH, USA, June.